Cell Reports
Article

Regulation of FAS Exon Definition and Apoptosis by the Ewing Sarcoma Protein

Maria Paola Paronetto,[1,2,3,*] Isabella Bernardis,[4] Elisabetta Volpe,[3] Elias Bechara,[1,4] Endre Sebestyén,[4] Eduardo Eyras,[4,5] and Juan Valcárcel[1,4,5,*]
[1]Centre for Genomic Regulation, carrer Doctor Aiguader 88, 08003 Barcelona, Spain
[2]University of Rome "Foro Italico," Piazza Lauro de Bosis 6, 00135 Rome, Italy
[3]Laboratories of Cellular and Molecular Neurobiology and of Neuroimmunology, Fondazione Santa Lucia, 00143 Rome, Italy
[4]Universitat Pompeu Fabra, carrer Doctor Aiguader 88, 08003 Barcelona, Spain
[5]Institució Catalana de Recerca i Estudis Avançats, Pg Lluis Companys 23, 08010 Barcelona, Spain
*Correspondence: mariapaola.paronetto@uniroma4.it (M.P.P.), juan.valcarcel@crg.eu (J.V.)
http://dx.doi.org/10.1016/j.celrep.2014.03.077

SUMMARY

The Ewing sarcoma protein EWS is an RNA and DNA binding protein implicated in transcription, pre-mRNA splicing, and DNA damage response. Using CLIP-seq, we identified EWS RNA binding sites in exonic regions near 5′ splice sites. A prominent target was exon 6 of the FAS/CD95 receptor, which is alternatively spliced to generate isoforms with opposing activities in programmed cell death. Depletion and overexpression experiments showed that EWS promotes exon 6 inclusion and consequently the synthesis of the proapoptotic FAS/CD95 isoform, whereas an EWS-FLI1 fusion protein characteristic of Ewing sarcomas shows decreased activity. Biochemical analyses revealed that EWS binding promotes the recruitment of U1snRNP and U2AF65 to the splice sites flanking exon 6 and therefore exon definition. Consistent with a role for EWS in the regulation of programmed cell death, cells depleted of EWS show decreased sensitivity to FAS-induced apoptosis, and elevated EWS expression enhances apoptosis in EWS-haploinsufficient Ewing sarcoma cells.

INTRODUCTION

The removal of introns from mRNA precursors is mediated by the spliceosome, a macromolecular machinery composed of uridine-rich small nuclear ribonucleoprotein particles (snRNPs, U1, U2, U4, U5, and U6) and more than 200 proteins that assemble on the pre-mRNA in a stepwise manner (Wahl et al., 2009). U1 and U2 snRNPs are involved in the initial recognition of the 5′ and 3′ splice sites (ss), respectively. U1 snRNP recognizes the 5′ splice site through base-pairing interactions with the 5′ end of U1 small nuclear RNA (snRNA), whereas three sequence elements at the 3′ end of the intron, the branchpoint, the polypyrimidine tract, and the 3′ ss AG, are recognized through the cooperative binding of the Branch point Binding Protein (BBP/SF1) and the 65 and 35 kDa subunits of the U2 Auxiliary Factor (U2AF). U2AF helps recruiting U2 snRNP to the branchpoint region, where base-pairing interactions with U2 snRNA define an adenosine residue that forms a 2′–5′ phosphodiester bond with the 5′ end of the intron after the first step of splicing catalysis (Wahl et al., 2009). Factors that initially recognize 5′ and 3′ splice sites can stabilize each other across the intron (intron definition) or across internal exons (exon definition), which in vertebrates are usually short compared with the length of the flanking introns (Gelfman et al., 2012).

Additional regulatory factors modulate splice-site recognition, including several families of RNA-binding proteins (RBPs) that are recruited to specific sequence elements present in exons or introns to enhance or silence splice-site utilization (Chen and Manley, 2009). The extent and direction of the effects of these sequences and cognate factors is often dependent on their location relative to the splice sites, thus generating RNA maps that can help to predict the relative use of competing splice sites (alternative splicing, AS) (Witten and Ule, 2011).

EWS protein belongs to the FET (FUS/TLS, EWS, and TAF15) family, which are closely related RBPs that can influence both transcription and RNA metabolism (Tan and Manley, 2009; Paronetto, 2013). Chromosomal translocations of the genes encoding these proteins are characteristic of certain cancers. For example, a translocation creating a fusion between EWS and the ETS transcription factor FLI-1 is frequent in cases of Ewing sarcoma (Delattre et al., 1992; Ross et al., 2013). FET proteins are composed of a DNA activation domain at the N terminus and an RNA-binding domain at the C terminus, comprising three arginine/glycine-rich (RGG) boxes and one consensus RNA Recognition Motif (RRM), which is the most conserved region within the family (Tan and Manley, 2009). It has been shown that EWS binds to poly U and poly G homoribopolymers (Ohno et al., 1994), and in vitro systematic evolution of ligands by exponential enrichment (SELEX) experiments identified GGUG as a motif recognized by FUS/TLS with 250 nM affinity (Lerga et al., 2001). EWS was also shown to recognize the G-rich single-stranded region of DNA or RNA G-quadruplex structures (Takahama et al., 2011).

Mounting evidence indicates that EWS participates in splicing of selected transcripts. EWS was initially shown to interact with the branchpoint recognizing protein BBP/SF1 (Zhang et al.,

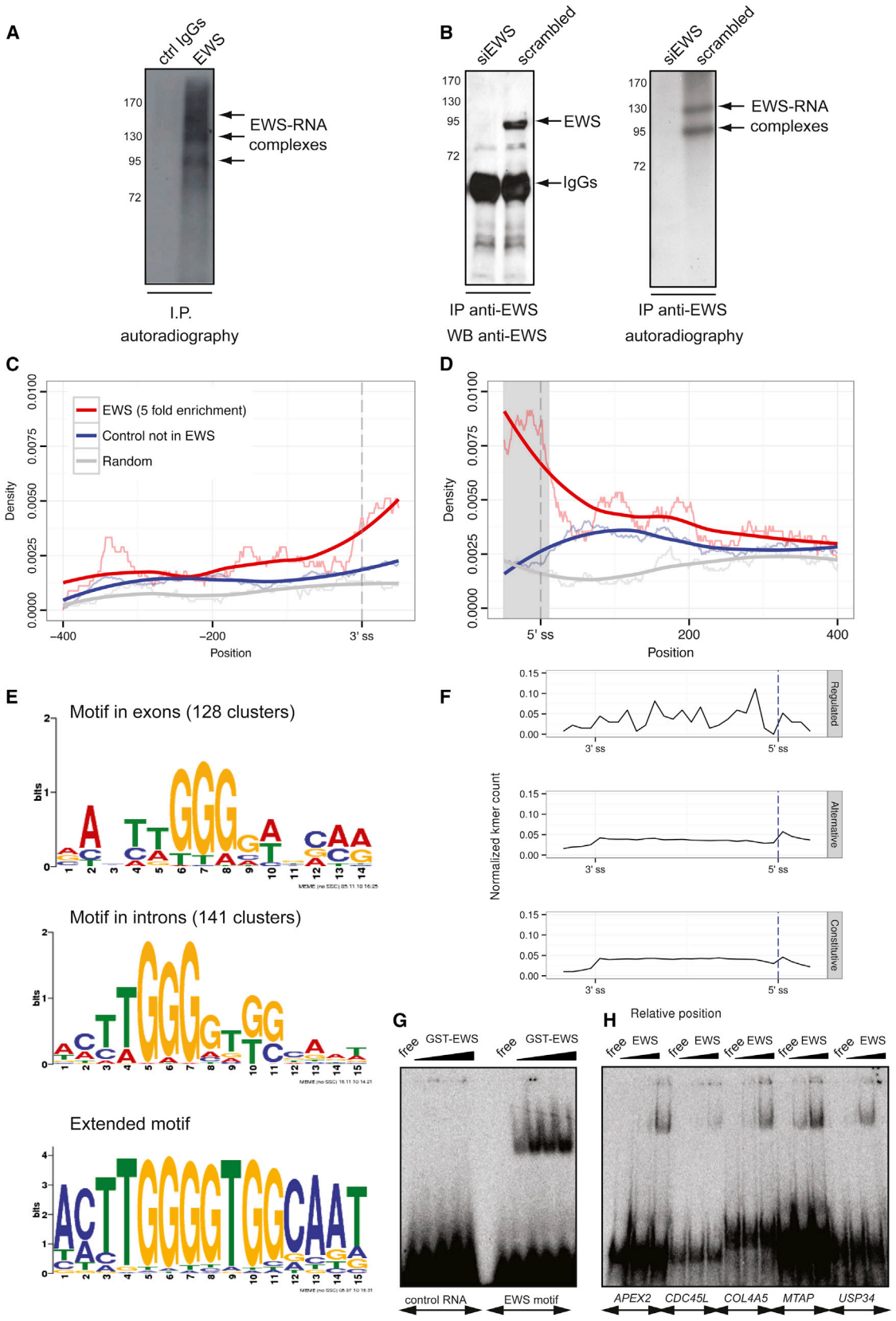

(legend on next page)

1998) and with U1C, one of the protein components of U1 snRNP (Knoop and Baker, 2000), suggesting a role in modulating 3′ and/or 5′ splice-site recognition. Indeed, EWS-FLI1 fusion protein, but not EWS alone, was shown to alter 5′ splice-site selection in the E1A model system (Knoop and Baker, 2000, 2001). Further work documented that EWS and EWS-FLI1 can promote transcription of cyclin D1 gene (*CCND1*) and that the two proteins have opposing effects in regulating the ratio between two alternatively spliced mRNA variants of *CCND1* with different oncogenic potential (Sanchez et al., 2008). Recent work has linked genotoxic stress with EWS-mediated regulation of AS. First, disruption of the interaction between EWS and the spliceosome-associated factor YB-1 induces skipping of several exons in the *MDM2* gene, which may contribute to proper p53 response (Dutertre et al., 2010). Second, EWS knockdown causes changes in AS of genes encoding factors important for the DNA damage response, which mimic changes in splicing induced by UV light irradiation (Paronetto et al., 2011). Notably, UV irradiation causes sequestration of EWS in the nucleolus, thus likely interfering with its splicing activity (Paronetto et al., 2011). However, the mechanisms by which EWS modulates splice-site selection remain largely unknown.

We report the genome-wide identification of EWS RNA targets by UV crosslinking and immunoprecipitation sequencing (CLIP-seq), their enrichment in exonic regions near 5′ splice sites, and a function for EWS in recruiting U1snRNP and U2AF to the flanking splice sites of the crosslinked target FAS/CD95 exon 6, enhancing exon inclusion and consequently FAS-mediated apoptosis.

RESULTS

CLIP Identifies EWS Binding Sites in a Variety of Transcripts

CLIP (ultraviolet light-induced crosslinking and immunoprecipitation) was used to identify in vivo RNA targets of EWS in HeLa cells in a genome-wide manner (see Experimental Procedures for details). EWS was immunoprecipitated from crosslinked HeLa extracts using either an antibody against EWS (Paronetto et al., 2011; Figure S1A), or purified rabbit immunoglobulin (IgGs) as a control (Figures 1A, S1A, and S1B). Depletion of EWS by RNAi strongly decreased the crosslinking detected in the immunoprecipitates, further arguing that the CLIP signal is specific (Figure 1B). Two independent replicate CLIP experiments were analyzed. A total of 2.9 million CLIP sequences were generated, 16% of which could be mapped to the human genome allowing 0–2 mismatches. Gene loci (9,274) with EWS CLIP tags in at least one replica were identified, and 4,994 gene loci had tags in both of the CLIP experiments. Total reads were clustered and the Pearson correlation between the two replicas using overlapping clusters (~8,000) was R = 0.801 (Figures S1C and S1G). Clusters overlapping between EWS and control IgGs were retained only if the number of reads corresponding to EWS clusters was at least five times higher than in control. Additionally, a set of "random" clusters was generated by selecting, for each EWS cluster, a new arbitrary location in the same chromosome, avoiding satellites, gaps, and overlaps with other random clusters. Although 70% of the clusters overlapping genes fall in introns, normalization by the relative length distribution of exons and introns revealed a 2-fold enrichment of EWS clusters in exons and promoter regions (Figure S1E). Sixty-two percent of these clusters fall in coding sequences (CDS), 27% in 3′ UTRs and 11% in 5′ UTRs, revealing a 30% enrichment of EWS clusters in CDS/internal exons (Figure S1F). Interestingly, a high density of crosslink sites was detected in different classes of noncoding RNAs, especially long intergenic noncoding RNAs (lincRNAs) and small nucleolar RNAs (snoRNAs; Figure S2 and Table S1), suggesting possible novel functions for EWS in the regulation of RNA metabolism.

Enrichment of EWS Binding Sites near 5′ Splice Sites

To identify functional signatures of EWS binding, the distribution of EWS CLIP-clusters relative to splice sites was investigated. A clear enrichment of EWS clusters over control and random clusters was found in exonic regions neighboring 5′ splice sites (compare red with gray/blue lines in Figure 1D; Figure S3). A

Figure 1. CLIP-Seq Identifies EWS Binding Sites in HeLa Cells Transcriptome

(A) Autoradiography of EWS immunoprecipitates from cellular extracts prepared from HeLa cells after UV light irradiation, using either an antibody against EWS or purified rabbit IgGs. After DNase and RNase treatments, RNAs coimmunoprecipitated with EWS and protected from enzymatic digestion were radioactively labeled and the immunoprecipitates fractionated by electrophoresis in SDS-polyadrylamide gels and exposed to film. The arrows indicate shifted bands corresponding to EWS bound to RNA fragments of different sizes (EWS/RNA complexes).

(B) Immunoprecipitation of EWS protein from HeLa nuclear extracts transfected with either siEWS or scrambled oligonucleotides, in normal (left panel) or CLIP high RNase (right panel) conditions. On the left panel, western blot analysis using anti-EWS antibody; the arrow indicates the position expected for EWS protein. On the right, autoradiography of P^{32}-labeled EWS-RNA complexes from EWS immunoprecipitates from UV-crosslinked HeLa cells. High RNase conditions were used. The positions of EWS and EWS-RNA crosslinked complexes are indicated.

(C and D) Cluster distribution at 3′ and 5′ splice sites. Positional distribution of EWS CLIP-seq clusters with at least 5-fold enrichment, relative to 3′ and 5′ splice sites (red line), compared with CLIP-seq clusters from control IgGs (blue line) and with a random set of sequences localized in the same chromosome of each EWS cluster (gray line). Shaded regions indicate positions where a statistically significant difference (p value <0.001) in was found between EWS and control clusters.

(E) Motif analysis of EWS CLIP-seq targets in exons and introns. Logos of positional nucleotide frequencies built from exonic or intronic clusters containing one or more enriched pentamer motifs. On the bottom, extended motif built from clusters with at least 5-fold enrichment compared to control reads.

(F) The plot represents the density of pentamers relative to the 5′ ss comparing 49 regulated exons with a (large) set of alternative and constitutive exons, including 50 nt of the flanking introns. The values in the y axis represent the frequency at which that relative position is occupied by one of the pentamers, normalized by the total number of exons to make them comparable across the three groups.

(G) Electrophoretic mobility shift assay (EMSA) using purified GST-EWS (250 nM) and P^{32} 5′ end-labeled RNA corresponding to the extended EWS motif (double copy) or a control sequence of the same length.

(H) Mobility shift assays using GST-EWS (0, 10, and 100 nM) and 5′ end-labeled RNAs corresponding to the CLIP tags identified in the indicated genes. Sequences are provided in Table S3.

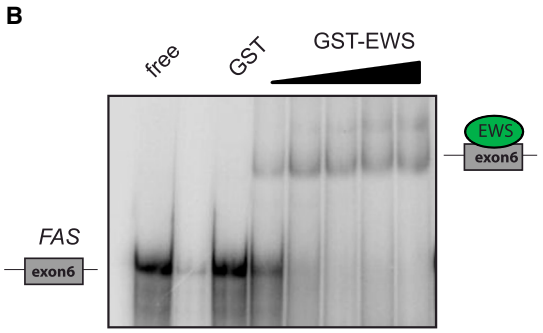

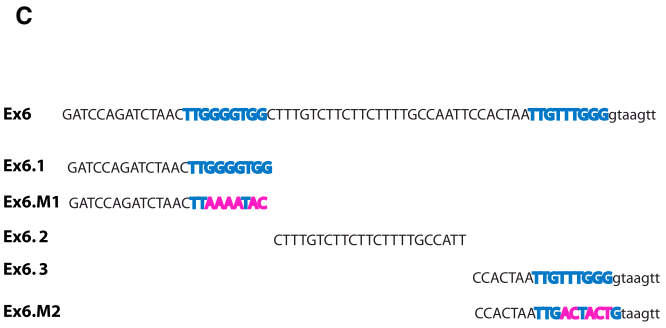

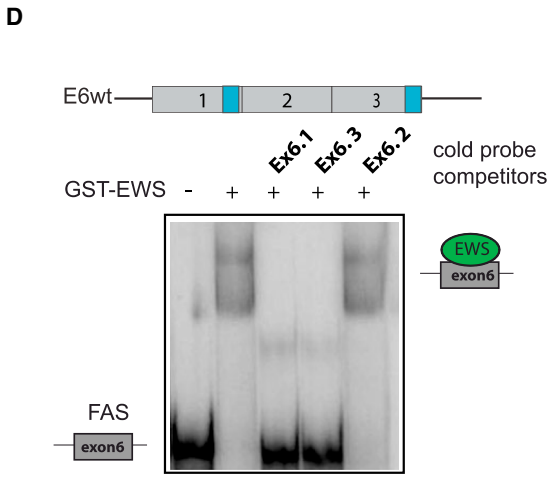

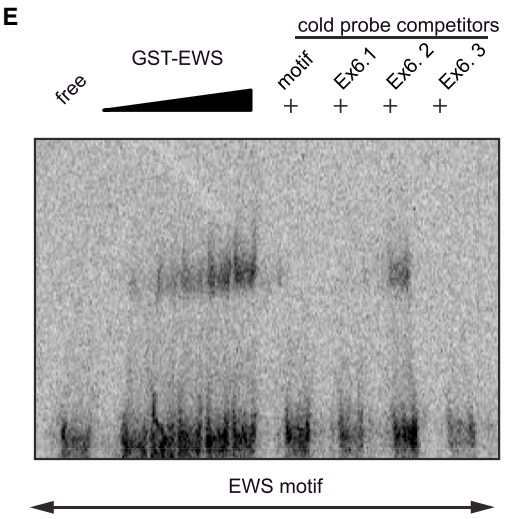

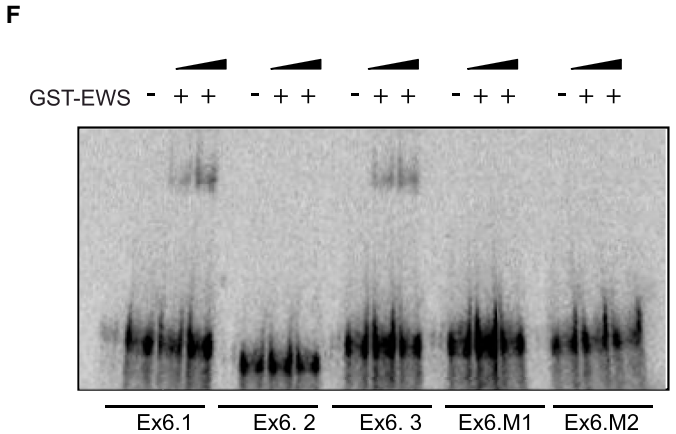

(legend on next page)

less pronounced enrichment could be also detected at exonic sequences flanking 3′ splice sites (Figure 1C). An enrichment of EWS clusters in weak 5′ (but not 3′) splice-site regions was observed, without significant differences between constitutive or alternative exons (Figures S3D–S3F). Additionally, we found that exons with CLIP clusters have in general weaker 5′ (but not 3′) splice sites than expected by chance (see Experimental Procedures).

EWS Binding Motif Analysis

To identify sequence motifs enriched in EWS CLIP clusters, which could represent sites of direct interaction by the protein, we searched for enriched k-mer (k = 5.6) motifs using two independent statistical tests, first calculating the number of times that each k-mer was represented in the clusters, and second calculating the number of clusters in which each k-mer is present. Each of these tests was performed comparing EWS versus control, as well as comparing EWS versus random. We selected 5-mers that had *Z* score $\geq$10 and chi score $\geq$100 in the two comparisons (Figures S4A and S4B) and those 6-mers that had *Z* score $\geq$15 and chi score $\geq$120 (Figures S4C and S4D) in the two comparisons (Table S2). Further analysis of the cluster containing these pentamers identified a GGGGT/A motif that was enriched in exons as well as in introns (Figures 1E and S4). In addition, an extended motif was found in clusters that were 5-fold enriched over control clusters (Figure 1E, lower panel) (see Experimental Procedures). Our results are consistent with previous reports describing G-rich motifs as high-affinity binding sites for FUS/TLS and EWS (Lerga et al., 2001; Takahama et al., 2011). The density of the pentamers was higher in EWS-regulated exons (see below) than alternative or constitutive exons not regulated by EWS, with the highest density within the exon's last quarter (Figures 1F and S5A). Analysis of the distribution of EWS clusters containing the pentamers confirmed an enrichment of the motif in exons, flanking/overlapping 5′ splice sites and less pronounced at 3′ splice sites (Figures S3G and S3H).

Binding of purified recombinant GST-EWS to P^{32}-5′-end-labeled RNAs corresponding to the identified consensus was observed in electrophoretic mobility shift assays (EMSAs), with an apparent dissociation constant around 50 nM, whereas no binding to a control sequence was detected (Figure 1G). This result argues that the CLIP data reflect intrinsic RNA binding features of the EWS protein. Consistently, direct binding of EWS to CLIP targets was confirmed by EMSA assays using ^{32}P-labeled RNA sequences corresponding to the CLIP tags identified in the genes *APEX2*, *CDC45L*, *COL4A5*, *MTAP*, and *USP34* (Figure 1H).

Identification of EWS-Regulated Genes

To identify genes regulated by EWS, we hybridized the RNA from three biological replicas of cells transfected with either scrambled or EWS small interfering RNA (siRNAs) to Affymetrix Human Exon Junction Arrays (HJAY) (Genosplice; see Experimental Procedures for details). The expression level of 805 genes was affected by EWS knockdown (395 upregulated and 410 downregulated), and more than half of these genes (425) contain CLIP tags, as determined by our CLIP-seq experiment (Figure S5C). These results suggest that association with EWS influences the accumulation of these target mRNAs. KEGG pathway analysis indicated that p53 signaling is the most represented pathway in EWS regulated genes (p value 2.46×10^{-6}), consistent with the previously proposed role for EWS in the regulation of stress response and DNA damage (Dutertre et al., 2010; Paronetto et al., 2011). HJAY identified 206 differentially regulated AS events in 114 genes; 68 regulated events contained CLIP tags within the alternatively spliced region. Interestingly, comparing the array design with the regulated AS events, we found a clear enrichment in cassette exon and alternative terminal exon events (Figure S5D).

Because the overlap between regulated exons and CLIP tags within the corresponding exonic sequences was limited, we used as a surrogate the presence of the identified EWS pentamers in 53 EWS-regulated internal exons. An enrichment of potential EWS binding sites in EWS-regulated exons compared to control exons, particularly near the 3′ end of the exon was observed (Figures 1F, S5A, and S5B), consistent with the general enrichment of CLIP tags observed in these regions (Figures 1C and 1D). RT-PCR analysis of eight array-predicted regulated exons containing potential EWS sites confirmed their regulation upon EWS depletion (Figure S5E; data not shown).

FAS as a Splicing Target of EWS Protein

To further study EWS function through exonic sequences as one possible mechanism of splicing regulation by this protein, we focused our attention on the most conspicuous CLIP cluster detected in the EWS CLIP-seq data, which corresponds to 408 reads spanning exon 6 (63 nucleotides) of the *FAS* pre-mRNA, and an additional cluster overlapping with part of exon 5 (Figure 2A). EMSA experiments confirmed direct binding of recombinant purified GST-EWS to *FAS* exon 6 pre-mRNA (from position −68 relative to the 3′ splice site of intron 5 to position +25 of intron 6), with an apparent *Kd* around 15 nM, an affinity higher than that determined for the EWS consensus motif (*Kd* 50 nM) (Figure 2B), consistent with the presence of two predicted

Figure 2. EWS Binds to *FAS* Pre-mRNA Sequences

(A) Representation of two highly populated EWS clusters identified in *FAS* pre-mRNA relative to the positions of exons 5 and the alternatively spliced exon 6.

(B) Mobility shift RNA binding assays using purified GST-EWS (10, 20, 40, 60, and 100 nM) and an RNA corresponding to *FAS* exon 6 and flanking intronic sequences (from −68 to +25). The positions of free RNA and RNA-protein complexes are indicated.

(C) Sequences of wild-type and mutant *FAS* pre-mRNA used for the mobility shift experiments.

(D) Upper panel: the location of two consensus motifs for EWS binding is represented relative to the three regions of *FAS* exon 6 indicated in (C). Lower panel: mobility shift competition assays using GST-EWS (100 nM), radioactively-labeled *FAS* exon 6 pre-mRNA (from −68 to +25), and nonlabeled RNAs corresponding to the regions of *FAS* exon 6 indicated in the upper panel and in (C).

(E) RNA binding assays using purified GST-EWS (10, 20, 30, 50, and 100 nM) and P^{32} 5′ end-labeled RNA corresponding to the extended motif revealed an apparent K_D of approximately 50 nM. EWS binding at 50 nM to the identified motif was challenged by competition with nonlabeled RNAs corresponding to the motif itself or corresponding to sequences of *FAS* exon 6.1 and 6.3, but not 6.2.

(F) Mobility shift binding assays using radioactively labeled RNAs corresponding to the regions of *FAS* exon 6 (wild-type or mutant) indicated in (C).

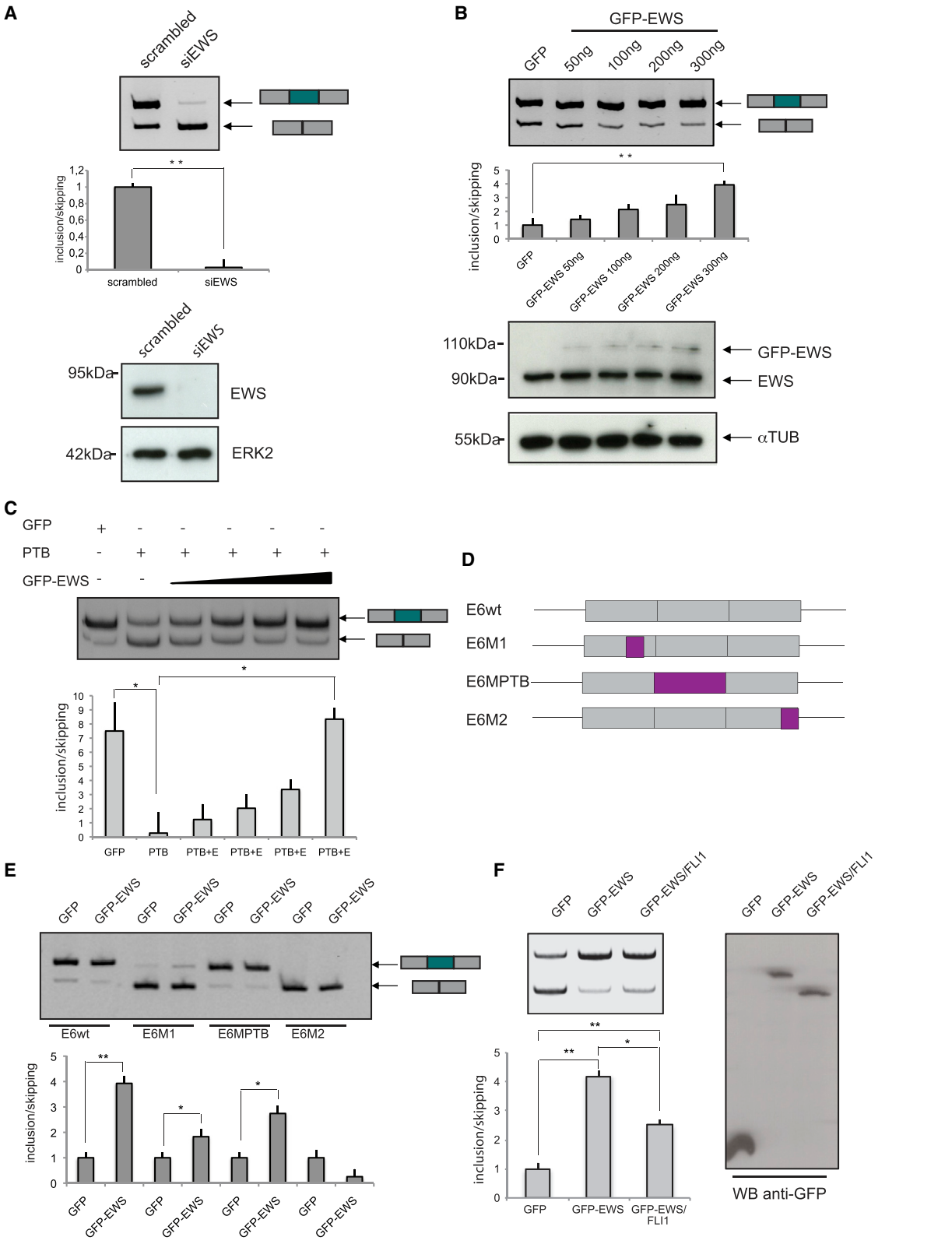

(legend on next page)

EWS binding motifs in this cluster (Figure 2C, blue lettering). To evaluate to what extent EWS binding to *FAS* exon 6 depends on these motifs, competition assays using 32P-labeled exon 6 pre-mRNA (−68 to +25) and unlabeled RNAs containing different fragments of the exon (Figure 2C) were carried out. Binding of EWS was competed by fragments Ex6.1 and Ex6.3 corresponding, respectively, to the 5′ third of *FAS* exon 6 and to the 3′ third of exon 6 and flanking 5′ splice site (Figure 2D). Both Ex6.1 and Ex6.3 contain EWS consensus sites, whereas fragment Ex6.2, which contains PTB binding sites (Izquierdo et al., 2005) but is devoid of putative EWS binding sites, did not compete (Figure 2D). Equivalent competition results were observed for EWS binding to the CLIP consensus motif (Figure 2E), further arguing that Ex6.1 and Ex6.3 do contain functional EWS binding motifs. The same conclusion was reached with binding assays using 32P-labeled Ex6.1, Ex6.2, and Ex.3 RNAs (Figure 2F). The apparent *Kd* for EWS binding to the Ex6.1 or Ex6.3 RNAs was 40–50 nM, significantly higher than the *Kd* for binding to *FAS* exon 6 region (15 nM), suggesting additive or possibly cooperative EWS binding when the two sites are present. To further confirm the contribution of EWS consensus sites, the G-rich stretches within putative EWS binding sites in Ex6.1 and Ex6.3 RNAs were mutated, to generate Ex6.M1 and Ex6.M2. Binding of EWS was significantly decreased by these mutations (Figure 2F), confirming the direct interaction of EWS with these sequences, consistent with the highly populated CLIP-seq cluster mapping to this region.

EWS Modulates *FAS* Alternative Splicing

To test whether EWS modulates splicing of *FAS* pre-mRNA, we knocked down expression of EWS in HeLa cells using siRNAs, which resulted in a significant decrease in protein expression (Figure 3A, lower panel). Using a human *FAS* exon 6 reporter minigene expressing the genomic region of the *FAS* gene spanning from exon 5 to exon 7 (Izquierdo et al., 2005), we observed that EWS knockdown resulted in a significant increase in exon 6 skipping compared to cells transfected with a scrambled sequence siRNA (Figure 3A, upper panel), measured by semiquantitative RT-PCR. The same tendency toward increased exon skipping was observed for endogenous *FAS* transcripts from a stable cell line infected with a lentivirus expressing EWS small hairpin RNAs (shRNAs), compared with a control-infected (pLKO) cell line (Figure S6A). EWS knockdown was also found to influence endogenous *FAS* exon 6 skipping in a genome-wide screen for regulators of this splicing event using a different set of siRNAs (J.R. Tejedor and J.V., unpublished data). Moreover, overexpression of increasing amounts of recombinant GFP-EWS in HeLa cells led to a steady increase in exon 6 inclusion from the *FAS* minigene (Figure 3B, upper panel).

Several factors were previously reported to regulate *FAS* AS: TIA-1 binds to uridine-rich sequences immediately 3′ of the 5′ splice site of intron 6, facilitating U1snRNP binding, 5′ splice-site recognition and exon inclusion (Förch et al., 2000, 2002; Izquierdo et al., 2005). On the other hand, the polypyrimidine tract binding protein (PTB) promotes exon skipping by binding to an exonic splicing silencer located in the central part of exon 6 and inhibiting exon definition (Izquierdo et al., 2005). Cotransfection of the *FAS* reporter minigene with a vector that allows PTB overexpression and increasing amount of GFP-EWS showed that EWS can counteract the effect of PTB and revert to substantial levels of exon 6 inclusion (Figure 3C). This effect was reproduced also using a minigene containing mutations in the TIA-1 responsive element (Figure S6B), indicating that EWS does not require this sequence element to promote exon inclusion.

To further delineate the sequence elements that mediate EWS function in *FAS* exon 6 inclusion, cotransfection assays were carried out using mutants in the EWS binding sites determined in Figure 2 (Figure 3D). Both mutations (specially mutant E6M2) caused higher levels of exon 6 skipping (compare lanes 1, 3, and 7 in Figure 3E). This result is consistent with a function for EWS in promoting *FAS* exon 6 inclusion, as described above, although we cannot rule out that the splicing enhancer effect associated with these sequences is not mediated, at least to some extent, also by additional cognate factors. GFP-EWS overexpression did not cause major increases in exon inclusion in these mutant constructs, despite the extensive levels of skipping observed in the absence of EWS overexpression (Figure 3E) and the potent reversion of exon skipping achieved by EWS under conditions of antagonism with PTB (Figure 3C). In particular, mutant E6M2 was completely unresponsive to EWS overexpression. Taken together, the results indicate that EWS acts through

Figure 3. Regulation of *FAS* Alternative Splicing by Changes in EWS Levels

(A) Effects of EWS knockdown on AS of FAS exon 6 reporter. siRNAs targeting EWS mRNA were transfected into HeLa cells cotransfected with a minigene corresponding to FAS genomic sequences between exons 5 and 7 and the levels of EWS protein determined by western blot analysis (lower panel) and the relative levels of FAS exon 6 inclusion/skipping determined from total RNA by RT-PCR using vector-specific primers (upper panel) and quantified by densitometric analysis of three independent experiments normalized to control scrambled siRNAs (middle panel).

(B) Effects of EWS overexpression on AS of FAS minigene. HeLa cells transfected with 0.3 μg of FAS minigene and the indicated amounts of a plasmid expressing GFP-EWS were harvested 20 hr after transfection, RNA isolated and FAS exon 6 inclusion/skipping levels determined by RT-PCR and quantified by densitometric analysis of three independent experiments normalized to the values of control, GFP-expressing cells (upper and middle panels). Expression of EWS and GFP-EWS was determined by western blot analysis (lower panel).

(C) EWS overexpression antagonizes the effects of PTB in regulation of FAS AS. HeLa cells transfected with 0.3 μg of FAS minigene were cotransfected with 0.3 μg of PTB-expressing plasmid and different amounts of GFP-EWS (50, 100, 200, and 300 ng) and ratios between inclusion and skipping of FAS exon 6 determined as in (C).

(D) Representation of FAS exon 6 wild-type and mutants used for cotransfections with GFP-EWS in (E). Purple boxes indicate the location of the regions mutated.

(E) Cotransfection assays of FAS minigenes and GFP-EWS were carried out and analyzed as in (C) using the constructs indicated in (D).

(F) EWS/FLI1 affects *FAS* AS. HeLa cells were transfected with 0.3 μg of *FAS* minigene and either GFP, or GFP-EWS, or GFP-EWS-FLI1 (300 ng). The ratio between *FAS* exon 6 inclusion versus skipping is indicated. Barplots represent quantification of three independent experiments. On the right, expression of the recombinant proteins (GFP, GFP-EWS, and GFP-EWS-FLI1) was determined by western blot analysis. Significance between the indicated distributions was evaluated using Student's t test: *$p < 0.05$, **$p < 0.01$, ***$p < 0.001$.

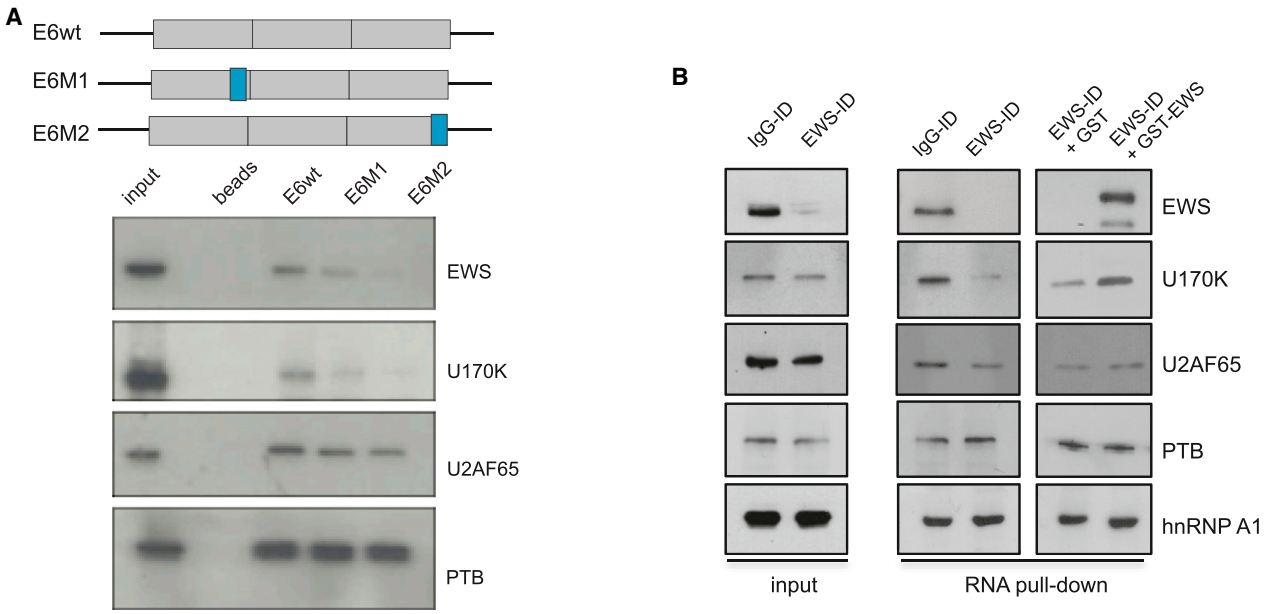

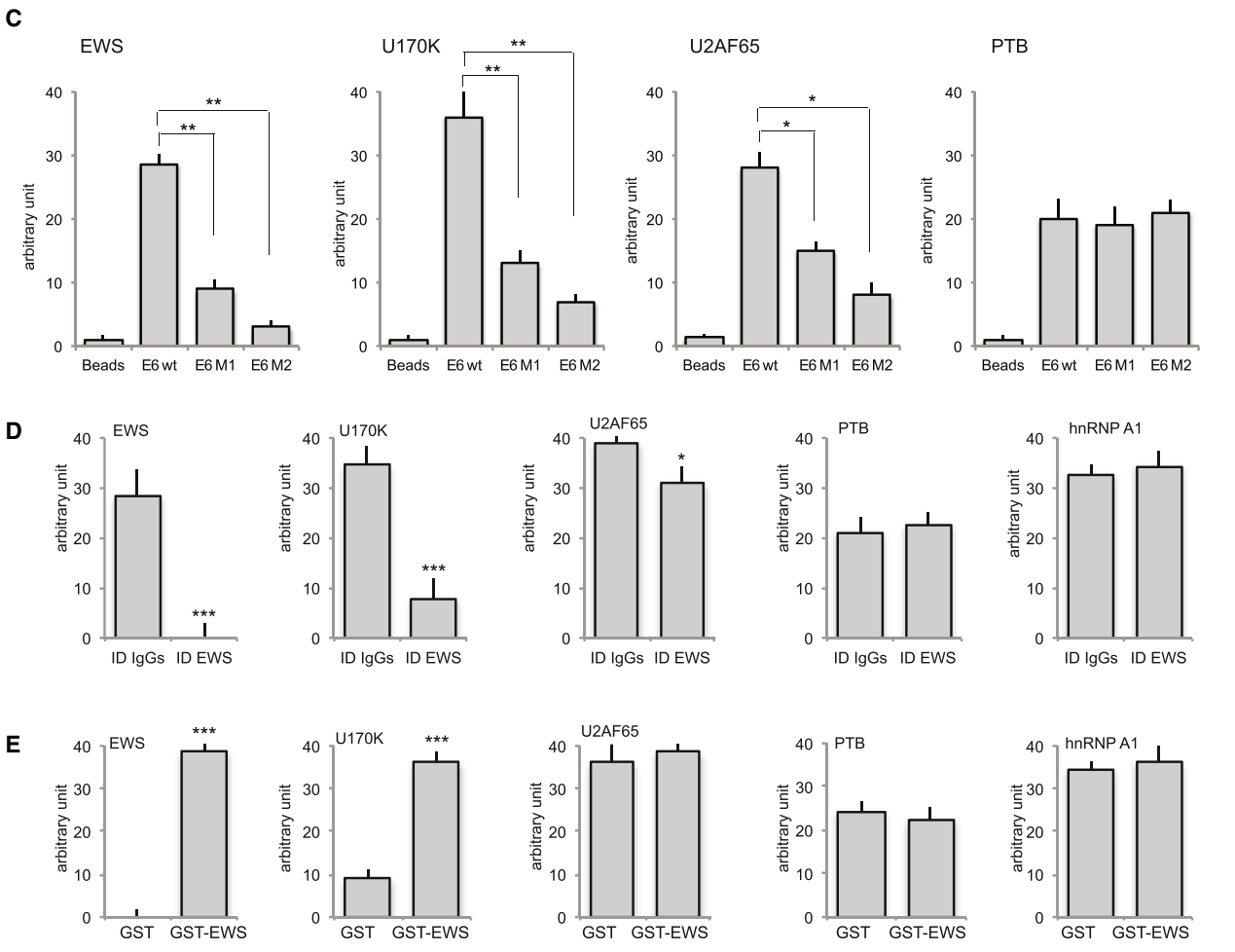

(legend on next page)

its binding sites in exon 6 (particularly the one closer to the 5′ splice site) to promote exon inclusion.

We previously showed that EWS is recruited to chromatin and can also directly bind single-stranded DNA (ssDNA) of target genes (Paronetto et al., 2011). Using chromatin immunoprecipitation (ChIP) assays, we observed association of EWS with the *FAS* gene and reduced residence time of RNA polymerase II (RNAPII) in the region upon EWS depletion (Figures S6C and S6D), which according to kinetic models of coupling between transcription and RNA processing (Kornblihtt, 2007) could contribute to EWS-mediated regulation of *FAS* exon 6. Results of RNA transfection experiments, however, indicated that coupling with transcription is not an essential requirement for EWS splicing regulation of *FAS* exon 6 (Figure S6E).

We next used similar cotransfection assays to test the activity of EWS-FLI1 fusion protein produced from the chromosomal translocation between the *EWSR1* and *FLI1* loci, characteristic of Ewing sarcomas (Delattre et al., 1992; Ross et al., 2013). Expression of the fusion protein in HeLa cells promoted exon 6 inclusion, albeit with about half of the efficiency of the wild-type EWS protein (Figure 3F). These results indicate that although the fusion does not block the splicing modulatory properties of EWS, it does compromise its full activity, opening the possibility that reduced levels of proapoptotic *FAS* isoform contribute to Ewing sarcoma tumor progression (see below and Discussion).

EWS Recruits U1 snRNP to *FAS* Exon 6 5′ Splice Site

Spliceosomal assembly is thought to occur through the sequential association and release of snRNPs on the pre-mRNA (Wahl et al., 2009). The ATP-independent binding of U1snRNP through base-pairing with the 5′ splice site and the recruitment of SF1 and U2AF65 to the branchpoint and polypyrimidine tract at the 3′ splice site are considered the earliest steps in spliceosome assembly and they correspond to the E or commitment complex. After formation of the E-complex, U2 snRNP stably associates with the branchpoint region in an ATP-dependent manner, which involves base-pairing interactions between U2 snRNA and sequences flanking the branchpoint adenosine, leading to the formation of the A complex (Wahl et al., 2009). Our observation that EWS clusters are enriched in the proximity of 5′ splice sites (Figure 1), together with the reported interaction of EWS with U1C in two-hybrid assays (Knoop and Baker, 2000), suggests a role for EWS in U1 snRNP recruitment to 5′ splice sites. To test this hypothesis, we carried out three types of experiments. First, we used affinity chromatography with wild-type *FAS* RNA (−68 to +25) and with mutant derivatives lacking either the EWS binding site within the 5′ third of exon (E6M1) or the binding site near the 5′ splice site (E6M2). Biotinylated RNAs were synthesized in vitro and incubated with HeLa nuclear extracts, and the complexes associated with the RNAs were pulled down using streptavidin beads. Proteins retained after stringent washes were eluted and analyzed by SDS-PAGE and western blot. We observed that EWS association with *FAS* exon 6 was decreased in the E6M1 mutant and was almost undetectable in the E6M2 mutant (Figure 4A, upper panel, see quantification in Figure 4C), consistent with the in vitro binding results of Figure 2 and with the requirement of these sites for EWS-mediated exon inclusion (Figure 3). Importantly, decreased binding of EWS correlated with reduced association of the U1 snRNP component U1 70K as well as with decreased association of U2AF65 (Figures 4A and 4C). In contrast, binding of PTB was not affected by the mutations. These observations correlate EWS binding to *FAS* exon 6 with the association of the splicing factors that mediate the earliest steps in the recognition of 5′ and 3′ splice sites.

To further substantiate these conclusions, we carried out RNA pull-down assays in nuclear extracts immunodepleted of EWS. Depletion of EWS resulted in significantly reduced association of U1 70K with *FAS* RNA (−68 to +25) and also in a mild reduction of U2AF binding, without effects on the association of PTB or hnRNP A1 (Figures 4B and 4D). Importantly, addition of recombinant purified EWS to the nuclear extracts restored U1 70K binding (Figures 4B and 4D), consistent with the proposed role of EWS in U1 snRNP recruitment. Despite the reduction in U2AF binding observed in EWS-depleted extracts, add-back of the protein did not significantly enhance U2AF association with the RNA, possibly because a factor required for exon definition was codepleted with EWS.

As an additional test, we evaluated the effect of adding an excess of GST-EWS to nuclear extracts in pull-down assays using RNAs with or without the 3′ or 5′ splice-site regions. As expected, U1 70K recruitment was reduced in the absence of 5′ splice site and, to a lower extent, in the absence of 3′ splice site. The association of U2AF was reduced in exon 6 RNAs lacking either the 3′ or the 5′ splice site (Figures 5A and 5B), consistent with previous work documenting that *FAS* exon 6 3′

Figure 4. EWS Binding Sites Regulate Binding of EWS as well as of Factors Involved in Exon Definition

(A) Pull-down assays of EWS, U170K, U2AF65, and PTB from HeLa nuclear extracts using biotinylated RNA corresponding to FAS exon 6 pre-mRNA and flanking intronic sequences spanning from −68 to +25. Wild-type and EWS binding site (in blue) mutant RNAs are represented in the upper panel. Pulled-down proteins were analyzed by western blot using antibodies against EWS, U1 70K, U2AF65, and PTB.

(B) Pull-down assays of HeLa nuclear extracts immunodepleted using either purified rabbit IgGs or anti-EWS antibody. The RNA pull-down was performed using in vitro transcribed biotinylated RNA corresponding to FAS exon 6 pre-mRNA and flanking intronic sequences spanning from −68 to +25 nucleotides as a bait. After extensive washes, pulled-down proteins were analyzed by western blot using antibodies against EWS, U170K, U2AF65, PTB, and hnRNP A1 (panels in the middle). On the right, pull-down experiment performed with EWS immunodepleted HeLa nuclear extracts rescued with either GST or GST-EWS recombinant protein purified from *E. coli*.

(C) Quantification of pull-down results in (A) by densitometric analysis. Bars indicate mean values ±SD of three independent experiments. Significance: binding to FAS mutated versus wild-type sequences were evaluated using Student's t test: *$p < 0.05$, **$p < 0.01$, ***$p < 0.001$.

(D and E) Quantification of pull down results in (B) by densitometric analysis. Bars indicate mean values ±SD of three independent experiments.

ID, immunodepleted; IgG, immunoglobulin. Significance was evaluated using the Student's t test (*$p < 0.05$, **$p < 0.01$, ***$p < 0.001$) for the binding of each protein to *FAS* pre-mRNA in IgG- versus EWS-immunodepleted nuclear extracts or in the immunodepleted extracts rescued with GST versus GST-EWS recombinant proteins.

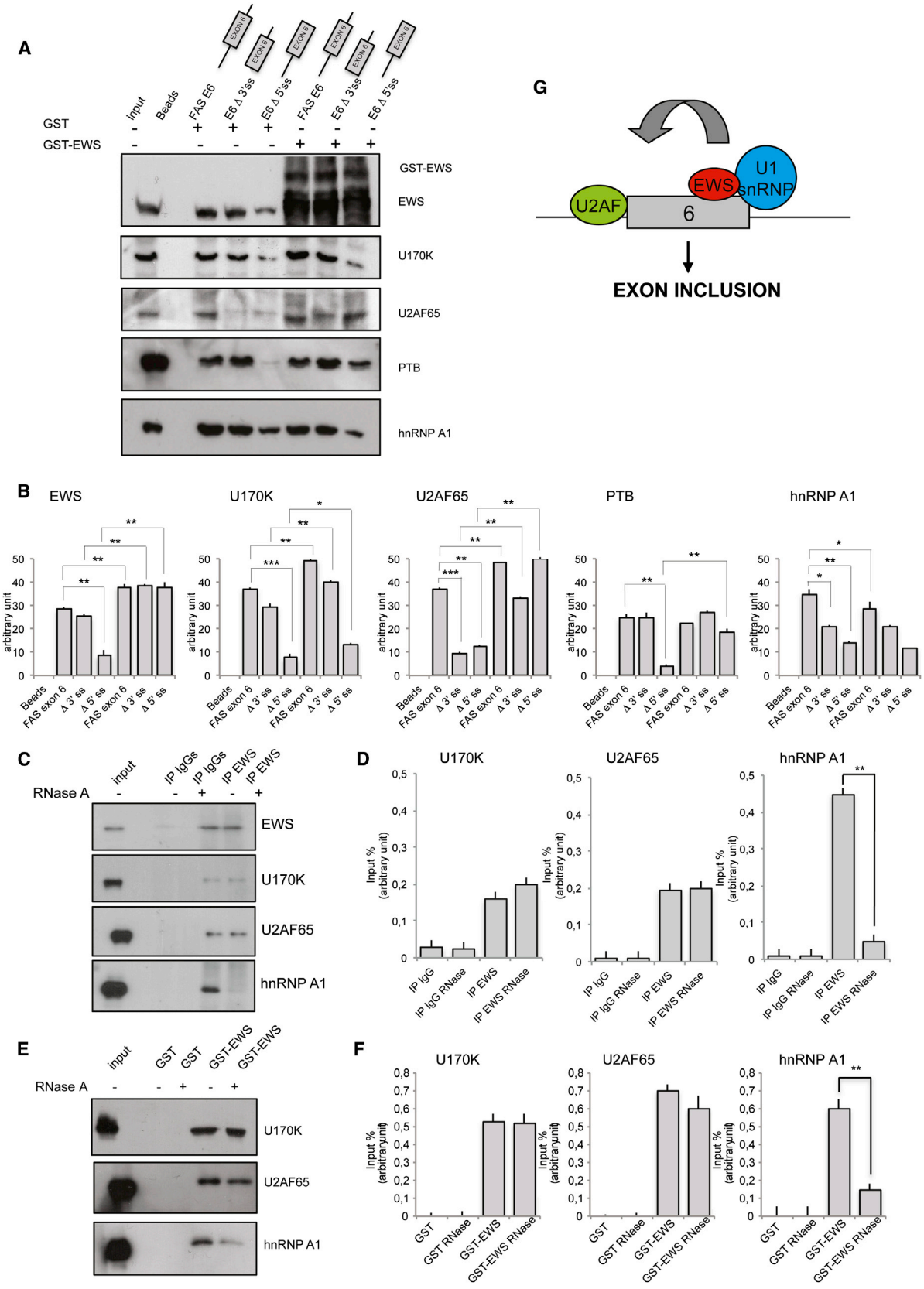

(legend on next page)

splice-site recognition is facilitated by interactions across the exon leading to exon definition (Izquierdo et al., 2005). Importantly, addition of GST-EWS enhanced the recruitment of both U1 70K and U2AF, whereas it did not enhance recruitment of PTB (except in the absence of 5′ splice site RNA, see Discussion) or hnRNP A1 (Figures 5A and 5B). Strikingly, enhanced recruitment of U2AF was observed even in the absence of a 3′ splice site, suggesting that EWS can help to recruit this factor, at least to some extent, in the absence of its cognate binding site. We also observed increased recruitment of U1 70K when adding back EWS in the absence of a 5′ splice site, but the effects were small and may not be of mechanistic significance. Coimmunoprecipitation assays showed that EWS forms complexes with U1 70K and U2AF in an RNase-insensitive fashion (Figures 5C and 5D), whereas coprecipitation of EWS with hnRNP A1 was sensitive to RNase A digestion. Furthermore, GST pull-down experiments confirmed the RNase-insensitive interaction between EWS and U1 70K and U2AF65 (Figures 5E and 5F). Collectively, these results suggest a direct role for EWS in the recruitment of U1 snRNP and, possibly, also U2AF and are compatible with a model in which EWS can favor exon recognition by promoting the recruitment of U1 snRNP to 5′ splice sites (Figure 5G, see Discussion) and also the recruitment of U2AF to 3′ splice sites, either directly or through exon definition effects (Figure 5G, see Discussion).

Reduced Sensitivity of EWS-Depleted Cells to FAS-Induced Apoptosis

FAS/CD95 encodes a *trans*-membrane receptor of the Death Receptor family. Upon binding to its ligand, the FAS receptor activates a signaling pathway that leads to apoptotic cell death (Mountz et al., 1995). Skipping of exon 6, however, leads to the synthesis of an mRNA that codes for a soluble form of the receptor known to repress apoptosis (Cheng et al., 1994; Cascino et al., 1995). EWS knockdown cells showed increased skipping of *FAS* exon 6, leading to the synthesis of the mRNA that encodes the soluble form of the *FAS* receptor. To evaluate the levels of FAS receptor in pLKO and pLKOshEWS cells, we performed staining with FAS antibody or matched isotype control antibody. Fluorescence-activated cell sorting (FACS) analysis confirmed a decrease in the levels of FAS receptor in pLKOshEWS HeLa cells compared to the pLKO control (Figures 6A and 6B).

Next, we evaluated the functional relevance of reduced expression of FAS receptor in EWS-knocked-down HeLa cells by inducing apoptosis with anti-FAS antibody. HeLa cells, stably infected with pLKO or pLKOshEWS, were treated for 16 hr with anti-FAS antibody or the matched isotype control antibody in Dulbecco's modified Eagle's medium (DMEM)-containing reduced serum. FACS analysis revealed that EWS depletion not only decreased the fraction of dead cells in the control population, but also reduced 2- to 3-fold the effects of FAS activation (Figures 6C and 6D). These effects of EWS depletion are unlikely to be due to a general increase in resistance to cellular challenges, because EWS-depleted cells are, in fact, more sensitive to genotoxic stress (Paronetto et al., 2011; Paronetto, 2013).

Ewing sarcomas are characterized by chromosomal translocations yielding in-frame fusions between the amino terminal region of EWS and the carboxy terminus of various ETS transcription factors, creating potent oncogenes that direct neoplastic transformation. As a consequence, in Ewing sarcoma cells the complete *EWSR1* gene is present only in one allele, potentially causing haploinsufficiency of EWS protein function. We therefore tested whether increasing the levels of EWS in Ewing sarcoma TC-71 cells could result in enhanced levels of FAS receptor and FAS-induced apoptosis. We overexpressed either GFP or GFP-EWS in TC-71 cells and measured the expression level of transmembrane FAS within GFP-positive cells by flow cytometry analysis. Although the whole population was positive for FAS receptor, we found a significant increase of the median fluorescence intensity (MFI) in GFP-EWS cells compared to the GFP control, indicating a 20% increase of FAS receptor molecules in GFP-EWS positive cells (Figures 6E and 6F). Consistent with the levels of EWS protein being rate limiting for FAS-induced apoptosis in Ewing sarcoma cells, treatment with anti-FAS inducer antibody for 16 hr in medium with reduced serum showed increased FAS-mediated cell death in GFP-EWS-expressing cells (Figure 6G). These cells showed increased cell

Figure 5. EWS Recruits U1 snRNP to *FAS* Exon 6 5′ Splice Site

(A) Pull-down assays of EWS, U170K, U2AF65, PTB, and hnRNP A1 from HeLa nuclear extracts using in vitro transcribed biotinylated RNA corresponding to *FAS* exon 6 pre-mRNA and flanking intronic sequences spanning from −68 to +25, or the same sequence without either the 3′ or the 5′ splice sites, as indicated. Pulled-down proteins were analyzed by western blot using antibodies against EWS, U170K, U2AF65, PTB, and hnRNP A1. ID, immunodepleted; IgG, immunoglobulin.

(B) Quantification of pull down results in (A) by densitometric analysis. Bars indicate mean values ±SD of three independent experiments. Significance: binding to *FAS* in the presence versus the absence of recombinant GST-EWS. Significance was evaluated using Student's t test: *$p < 0.05$, **$p < 0.01$, ***$p < 0.001$.

(C) Analysis of EWS interaction with U170K and U2AF65. Nuclear extracts from HeLa cells were immunoprecipitated either with anti-EWS antibody or purified rabbit IgGs, in the presence or absence of RNase A. Immunoprecipitated proteins were analyzed by western blot using antibodies against EWS, U170K, U2AF65, and hnRNP A1.

(D) Barplots represent average and SD of three independent immunoprecipitation experiments. Interaction with endogenous EWS protein is represented as percentage of the input. Significance was evaluated using the Student's t test (*$p < 0.05$, **$p < 0.01$, ***$p < 0.001$) comparing the binding in the presence or absence of RNase A.

(E) GST pull-down experiments using GST and GST-EWS proteins purified from *E. coli*. Pulled-down proteins were analyzed by western blot using antibodies against U170K, U2AF65, and hnRNP A1, as indicated.

(F) Barplots represent average and SD of three independent pull-down experiments. Interaction with GST or GST-EWS is represented as percentage of the input. Significance was evaluated using the Student's t test as in (D).

(G) Model for EWS-mediated effects on exon definition. EWS binding to G-rich elements in exons in the vicinity of 5′ splice sites helps to recruit U1 snRNP, particularly to weak 5′ splice sites, most likely involving interactions with the U1 snRNP protein U1C (Knoop and Baker, 2000). Enhanced binding of U1 snRNP to the 5′ splice site can promote U2AF65 binding to the upstream 3′ splice site through exon definition effects.

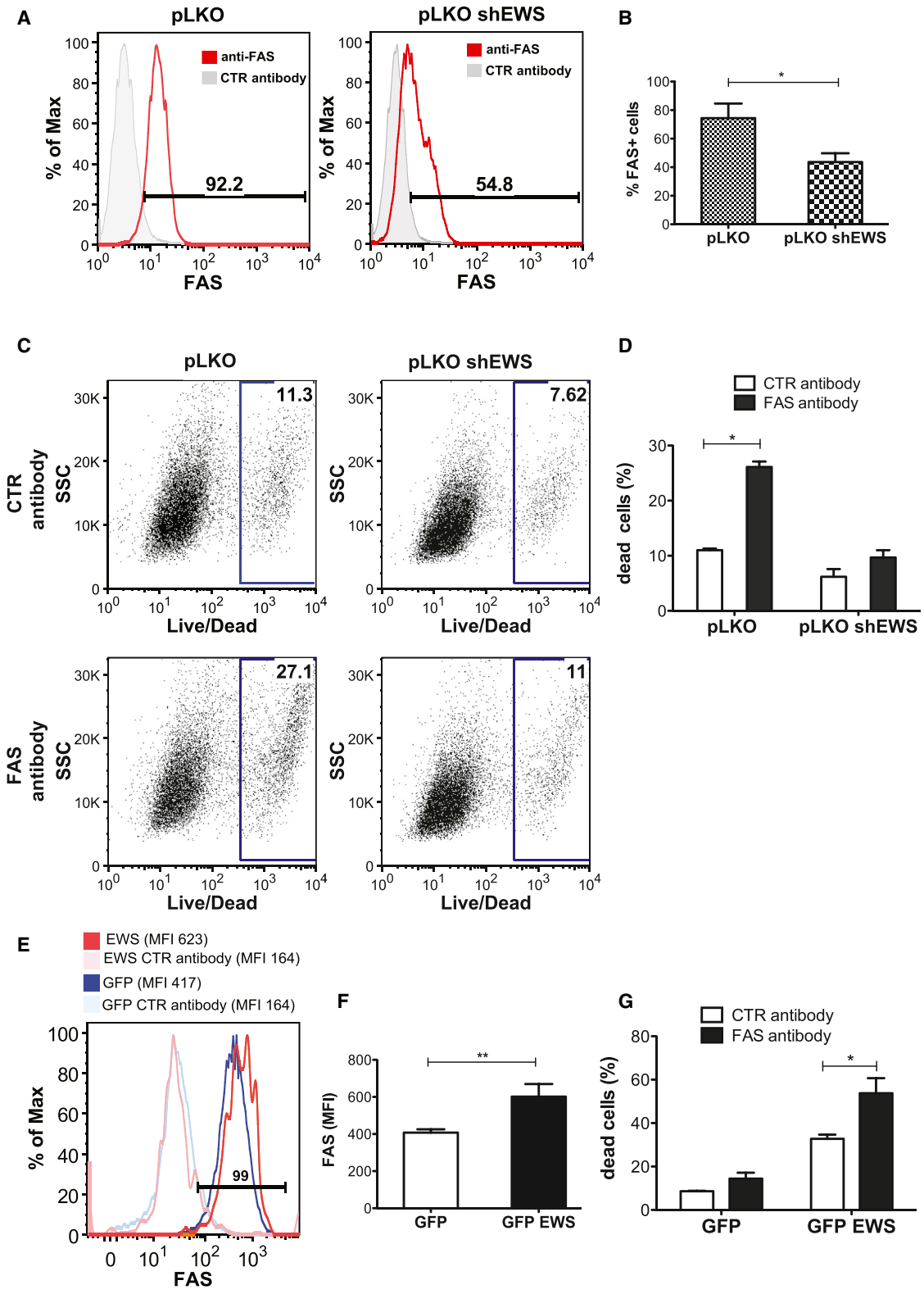

Figure 6. EWS Sensitizes Cells to FAS-Induced Cell Death

(A) EWS affects expression of membrane-bound FAS receptor in HeLa cells. The percentage of FAS-positive cells in HeLa cells stably infected with pLKO or pLKOshEWS was determined by flow cytometry comparing the percentage of cells stained either with the fluorescent anti-FAS (red line) or the matched isotype control antibody (gray line).

(legend continued on next page)

death even in the absence of inducer, suggesting increased response to apoptotic signals in the medium.

Collectively, the results of our EWS depletion and overexpression experiments indicate that EWS levels modulate the response to FAS-mediated apoptosis, both in ovarian cancer HeLa cells and in Ewing sarcoma cells.

DISCUSSION

The application of CLIP-seq/HITS-CLIP technology is providing comprehensive data sets of binding sites for a number of RNA binding proteins, including splicing regulatory factors (reviewed by Darnell, 2010). Our results reveal enrichment in EWS binding sites at exonic positions near 5′ splice sites (Figure 1). Consistently, the general consensus motif derived from EWS CLIP tags, which matches previous knowledge about EWS RNA binding specificity and for which purified EWS displays an apparent dissociation constant of 50 nM (Figure 1G), is also enriched at these locations (Figure 1F). Previous PAR-CLIP data reported a general enrichment of FET proteins immediately upstream of 3′ splice sites (Hoell et al., 2011). Our experiments, particularly using the *FAS* exon 6 as a model system, are consistent with bona fide EWS binding to exonic sequences near 5′ splice sites and with function of the protein through these sequence motifs (Figures 2, 3, and 4).

Enrichment of EWS binding near 5′ splice sites is consistent with a role for this protein in facilitating 5′ splice-site recognition (Figure 5H), a mechanism with similarities to the function of TIA-1/TIAR proteins in promoting 5′ splice-site choice and exon definition. First, both proteins bind to sequences located near 5′ splice sites, although TIA-1/TIAR bind to uridine-rich sequences 3′ of the splice site and EWS binds to guanosine-rich sequences 5′ of the splice site. This arrangement opens the possibility that 5′ splice-site recognition can be assisted by both TIA-1/TIAR and EWS proteins, which could act synergistically through independent binding sites flanking the splice site. In *FAS* exon 6, the effect of EWS is not affected by mutation of the TIA-1 binding site (Figure S6), indicating that synergy between EWS and TIA-1 is not a requirement for EWS function in this case. Second, both proteins interact with U1C, one of the protein components of U1 snRNP (Förch et al., 2002; Knoop and Baker 2000) which in budding yeast has been shown to recognize 5′ splice-site sequences previous to base-pairing interactions between the splice site and U1 snRNA (Du and Rosbash 2002). Third, both TIA-1 (Förch et al., 2000; Izquierdo et al., 2005) and EWS (Figures 4 and 5) promote U1 snRNP assembly. Taken together, these similarities suggest a model in which recognition of sequences flanking 5′ splice sites by EWS and/or TIA1/TIAR proteins helps to recruit U1 snRNP through their interaction with U1C. Such stabilizing contacts are likely to play a more determinant role near weak 5′ splice sites, where suboptimal base-pairing interactions with U1 snRNA will make U1 snRNP recruitment more dependent on auxiliary sequences and factors like TIA-1 and EWS (Förch et al., 2000; Wang et al., 2010; Figures S3C and S3D). These interactions, as well as others reported in the literature (e.g., between the SR protein SRSF1 and U1 70K; Kohtz et al., 1994; Jamison et al., 1995) can be important for constitutive recognition of 5′ splice sites and also for regulation of AS (Wang et al., 2010). Previous work documented that guanosine runs adjacent to weak 5′ splice sites can buffer effects of 5′ splice-site mutations, allowing polymorphisms and evolution of new splicing patterns (Xiao et al., 2009). Although the effects of these sequences were linked to the activity of hnRNP H (Xiao et al., 2009), the results presented here argue that EWS can be an additional mediator of these effects.

Increased recruitment of U2AF by EWS (Figures 4 and 5) could be an indirect consequence of EWS-mediated enhanced U1 snRNP binding, which facilitates U2AF binding to *FAS* exon 6 3′ ss through exon definition (Izquierdo et al., 2005). The results of Figure 5 suggest an additional mechanism, whereby EWS interacts (directly or through intermediate factors) with U2AF. Thus, EWS can promote the recruitment of the earliest factors recognizing 3′ and 5′ splice sites (U2AF and U1 snRNP) and therefore act itself as a mediator of exon definition. Although clear effects on U2AF recruitment were observed upon mutation EWS binding sites or upon addition of an excess of EWS to nuclear extracts, the effects of EWS depletion/add back were less clear. One possibility to explain these observations is that EWS was not depleted sufficiently to strongly compromise U2AF binding in these assays. Although we found that coupling with transcription is not an absolute requirement for EWS function on *FAS* AS, the slower transit of RNAPII observed in the presence of EWS (Figure S6) could contribute to regulate *FAS* AS by providing a longer window of opportunity for the recruitment of splicing factors on the regulated exon (Kornblihtt, 2007). EWS could therefore facilitate exon definition via transcriptional coupling and through coupling-independent mechanisms. The EWS cluster in *FAS* exon 6 contains two motifs that match EWS binding consensus (Figure 2). EWS binds *FAS* exon 6 with an apparent K_D of 15 nM, indicating about 3-fold higher affinity for this sequence than for the identified

(B) Quantification of FACS analysis results obtained as in (A) for three independent experiments.

(C) EWS facilitates FAS-mediated cell death of HeLa cells. pLKO and pLKOshEWS stable HeLa cell lines were treated with anti-FAS inducer antibody or with matched isotype control antibody for 16 hr in DMEM with reduced serum content (1%) and the fraction of dead cells determined by staining with the live/dead fixable near infrared reagent and analyzed by FACS. The percentage of live/dead positive cells (in blue rectangles) corresponds to percentage of dead cells.

(D) Quantification of results as in (C) for three independent experiments.

(E) EWS enhances expression of membrane-bound FAS in Ewing sarcoma TC-71 cells. TC-71 cells were transfected with either GFP- or GFP-EWS-expressing plasmids and 48 hr after transfection cells were stained with fluorescent anti-FAS antibody, analyzed by flow cytometry. We analyzed the percentage of FAS positive cells and the median fluorescence intensity (MFI) between GFP-EWS and GFP control cells within GFP-positive cells.

(F) Quantification of MFI results as in (E) corresponding to three independent experiments.

(G) EWS facilitates FAS-mediated cell death of Ewing sarcoma TC-71 cells. TC-71 cells transfected either with GFP- or with GFP-EWS-expressing plasmids were treated with anti-FAS inducer antibody or with the matched isotype and the percentage of dead cells analyzed as in (C). The barplot represents the average and SD of three independent experiments. Significance was evaluated using the Student's t test (*$p < 0.05$, **$p < 0.01$, ***$p < 0.001$).

extended consensus motif itself. This could be explained by additive or cooperative effects of EWS association with the two motifs present in the exon. Mutation of each of these elements reduces EWS binding (Figure 2) and reduces the effects of EWS overexpression on *FAS* exon 6 inclusion (Figure 3), again suggesting functional synergy between EWS proteins through the two binding sites in this rather short (63 nucleotides) exon. Consistent with this notion, mutation of each EWS consensus motif leads to substantial skipping of *FAS* exon 6 (Figure 3) and an excess of EWS added to extracts greatly enhances the recruitment of the endogenous EWS protein as well (Figure 5).

Chromosomal translocation of the *EWSR1* locus to genes encoding ETS transcription factors, frequently FLI1, generates fusion proteins that have been shown to have abnormal properties as transcriptional activators in Ewing sarcoma, liposarcoma, and chondrosarcoma (Delattre et al., 1992; Ross et al., 2013). EWS-FLI1 retains the ability to interact with U1C (Knoop and Baker, 2000) and has been shown to counteract the 5′ splice-site switching effects of hnRNP A1 on an E1A AS model (Knoop and Baker, 2001). It remains possible that part of the pathogenic effects associated with the genetic lesion characteristic of Ewing sarcomas are the result of haploinsufficiency of EWS or of altered properties of EWS-FLI1 as a splicing regulator. The results of Figure 3F are consistent with this idea, because they show lower activity of the EWS-FLI1 in the regulation of *FAS* splicing. In this regard, it has been shown that, whereas both the EWS and EWS-FLI1 promote *CCND1* gene expression, EWS-FLI1 decreases RNAPII elongation rate and favors accumulation of the more oncogenic D1b isoform (Sanchez et al., 2008), illustrating how the distinct function of these proteins in coupling of transcription and RNA processing can contribute to tumor progression.

The identification of *MDM2* (Dutertre et al., 2010), of genes encoding factors involved in DNA damage response (Paronetto et al., 2011), and of *FAS* (this manuscript) as targets of splicing regulation by EWS provides possible pathogenic mechanisms by which a decrease in activity (or dominant-negative effects) caused by *EWSR1* translocations lead to unbalanced p53 activity, genome instability, or/and decreased apoptosis, thus contributing to tumor progression. On the other hand, we found here that forced expression of EWS in the TC-71 Ewing sarcoma cells is sufficient to increase FAS levels in the membrane and, consequently, FAS-mediated cell death. AS of *FAS* exon 6 is indeed important for normal B and T cell differentiation and for the proliferation of cancer cells (Cascino et al., 1995; Cheng et al., 1994). A detailed comparison between the activities of EWS and its pathogenic fusion proteins is likely to provide relevant insights in this regard. Interestingly, a small molecule that blocks the interaction between EWS-FLI1 and RNA helicase A (which has activities in the splicing process) was found to induce apoptosis of Ewing sarcoma cells (Erkizan et al., 2009).

In summary, our results reveal a molecular mechanism by which EWS can promote U1 snRNP recruitment to weak 5′ splice-sites and exon recognition. They also establish a connection between EWS and FAS-mediated apoptosis, which could be relevant for the pathogenesis mechanisms behind Ewing and other sarcomas.

EXPERIMENTAL PROCEDURES

CLIP Experiments and Data Processing

CLIP experiments were performed as previously described (Chi et al., 2009; Supplemental Information). Solexa 36 nucleotide reads from EWS precipitates (2914302) and from control precipitates (2947185) were mapped to the human genome using GEM (Marco-Sola et al., 2012), allowing for up to two mismatches and retaining only sequences that mapped uniquely to the genome. All the unmapped reads were then trimmed 1 base from the 3′ end and remapped. This sequential trimming and mapping was continued up to 21 nt length reads (15 bases of trimming). As a result, a total of 467,818 EWS-associated reads and 687,823 control reads were unambiguously mapped, which were grouped in 97,011 and 72,883 clusters, respectively, allowing an overlap of one or more nucleotides. Two rankings for EWS clusters were considered: not in control clusters, which are built from overlapping CLIP reads after removing all those that overlap any of the control reads, and 5-fold enriched clusters, which are defined to have five times or more reads than the control cluster. Five-fold enriched clusters were calculated after one pseudocount was added to all clusters regions in both samples.

Calculation of Cluster Density Relative to Splice Sites

For each data set (C), we calculated the density $d(x)$ of clusters falling in a particular position x relative to the splice sites as follows: $d(x) = (n(x)/N) \cdot (CE/C)$, where $n(x)$ is the number of exons that have a cluster in that position, N is the total number of exons considered that have clusters on either side, and CE/C is the proportion of clusters of this set that fall nearby exons. To calculate the density of EWS clusters near weak/strong splice sites for constitutive exons, a position weight-matrix was built using real sites (RefSeq genes acceptors and donor sites) and random sites (random intergenic regions containing AG and GT; 18bp-AG-3bp and 3bp-GT-4bp). Exons were scanned using the matrix and each site classified as weak or strong if it was in the bottom 25% or top 25% of the ranking of scores, respectively. Reciprocally, the association of weak and strong splice sites with EWS clusters was studied using an independent calculation: 3′ and 5′ splice sites of exons were scored with SVM_BP (Corvelo et al., 2010) and MaxEntScan (Yeo and Burge, 2004), respectively. The distribution of splice-site scores was compared between exons with clusters and all exons. One thousand iterations were performed, sampling the same number of exons from each set, and a Kolmogorov-Smirnov test was performed to compare both distributions at each iteration. Maximal p values obtained for the 1,000 comparisons of 5′ splice sites were 2.596×10^{-09} for 5-fold enriched CLIP clusters and 0 for CLIP clusters not in control. For the 3′ splice sites, maximal p values were 0.988 for 5-fold enriched clusters and 0.117 for clusters not in control. Finally, to test the significant differences in cluster densities at each position, a Fisher' exact test was carried out using the $n(x)$ and $C - n(x)$ values for the "EWS not in control" and "EWS (5-fold enrichment)" versus "control not in EWS" comparison, and using the $n(x)$ and $N - n(x)$ values for the case of "EWS not in control – strong acceptor/donor" versus "EWS not in control – weak acceptor/donor" and "EWS not in control – alternative exon" versus "EWS not in control – constitutive exon" comparison. The Fisher p values were adjusted with the Benjamini-Hochberg method, and only positions with adjusted p values <0.001 are shown as gray-shaded areas.

Motif Analysis

Two statistical tests were performed using pentamers: a Z score test to obtain pentamers overrepresented in CLIP clusters relative to the set of control clusters and the set of random clusters, and a c^2 test to obtain pentamers that occur in a significant number of CLIP clusters compared to the other two sets. We considered as significant those 5-mers that had Z score ≥ 10 and chi score ≥ 100 in the two comparisons (Figures S4A and S4B) and those 6-mers that had Z score ≥ 15 and chi score ≥ 120 (Figures S4C and S4D). Those k-mers that were common and significant in all four tests were then kept for further analysis (Table S2). Similar analyses were performed comparing k-mers (k = 5.6) in control clusters versus random clusters using the same thresholds; none of the enriched k-mers in these comparisons coincided with the ones for EWS (Figures S4E and S4F). The significant k-mers were then located in the CLIP clusters. For positions with at least two pentamers

overlapping, 25 nt of sequence centered at the overlapping pentamers was extracted for each CLIP cluster. The best 1,000 clusters according to pentamer count were then analyzed with MEME (http://meme.nbcr.net/meme/) to obtain a sequence-logo, searching for 0–1 motif/sequence and for motifs of maximal length of 15 nucleotides occurring in a minimum of 40 sequences.

Splicing-Sensitive Microarray Experiments

RNA from three biological replicates of scrambled or siEWS-transfected HeLa cells was isolated and DNase digested using the RNeasy kit (QIAGEN). Total RNA was hybridized to Human Affymetrix Exon-Junction Array (HJAY). The HJAY data set analysis and visualization were carried out using EASANA (GenoSplice technology, http://www.genosplice.com), based on the FAST DB annotation.

Additional and standard methodology for biochemical and cellular assays are detailed in Supplemental Experimental Procedures.

ACCESSION NUMBERS

CLIP and microarray data have been submitted to the GEO database with accession numbers GSE47431 and GSE47790, respectively, and are also available at this site: http://regulatorygenomics.upf.edu/Data/EWS/.

SUPPLEMENTAL INFORMATION

Supplemental Information includes Supplemental Experimental Procedures, six figures, and three tables and can be found with this article online at http://dx.doi.org/10.1016/j.celrep.2014.03.077.

ACKNOWLEDGMENTS

We thank Sophie Bonnal, Anna Corrionero, Juan Ramón Tejedor, Camilla Iannone, and Nicolás Bellora for helpful suggestions and reagents. M.P.P. was supported by a fellowship from the HFSP. This project was supported by Fundación Botín, Fundación Sandra Ibarra (FSI2013), the European Union Sixth Framework Programme under grant agreement Nr. LSHG-CT-2005-518238-V (EURASNET), the Spanish Ministry of Economy and Competitiveness (grant no. CSD2009-00080, Consolider RNAREG/BFU2011-29583 / BIO2011-23920), and AIRC (Grant MFAG 11658). We also acknowledge support of the Spanish Ministry of Economy and Competitiveness, "Centro de Excelencia Severo Ochoa 2013-2017" (SEV-2012-0208).

Received: August 6, 2013
Revised: February 16, 2014
Accepted: March 31, 2014
Published: May 8, 2014

REFERENCES

Cascino, I., Fiucci, G., Papoff, G., and Ruberti, G. (1995). Three functional soluble forms of the human apoptosis-inducing Fas molecule are produced by alternative splicing. J. Immunol. *154*, 2706–2713.

Chen, M., and Manley, J.L. (2009). Mechanisms of alternative splicing regulation: insights from molecular and genomics approaches. Nat. Rev. Mol. Cell Biol. *10*, 741–754.

Cheng, J., Zhou, T., Liu, C., Shapiro, J.P., Brauer, M.J., Kiefer, M.C., Barr, P.J., and Mountz, J.D. (1994). Protection from Fas-mediated apoptosis by a soluble form of the Fas molecule. Science *263*, 1759–1762.

Chi, S.W., Zang, J.B., Mele, A., and Darnell, R.B. (2009). Argonaute HITS-CLIP decodes microRNA-mRNA interaction maps. Nature *460*, 479–486.

Corvelo, A., Hallegger, M., Smith, C.W., and Eyras, E. (2010). Genome-wide association between branch point properties and alternative splicing. PLoS Comput. Biol. *6*, e1001016.

Darnell, R.B. (2010). HITS-CLIP: panoramic views of protein-RNA regulation in living cells. Wiley Interdiscip Rev RNA *1*, 266–286.

Delattre, O., Zucman, J., Plougastel, B., Desmaze, C., Melot, T., Peter, M., Kovar, H., Joubert, I., de Jong, P., Rouleau, G., et al. (1992). Gene fusion with an ETS DNA-binding domain caused by chromosome translocation in human tumours. Nature *359*, 162–165.

Du, H., and Rosbash, M. (2002). The U1 snRNP protein U1C recognizes the 5′ splice site in the absence of base pairing. Nature *419*, 86–90.

Dutertre, M., Sanchez, G., De Cian, M.C., Barbier, J., Dardenne, E., Gratadou, L., Dujardin, G., Le Jossic-Corcos, C., Corcos, L., and Auboeuf, D. (2010). Cotranscriptional exon skipping in the genotoxic stress response. Nat. Struct. Mol. Biol. *17*, 1358–1366.

Erkizan, H.V., Kong, Y., Merchant, M., Schlottmann, S., Barber-Rotenberg, J.S., Yuan, L., Abaan, O.D., Chou, T.H., Dakshanamurthy, S., Brown, M.L., et al. (2009). A small molecule blocking oncogenic protein EWS-FLI1 interaction with RNA helicase A inhibits growth of Ewing's sarcoma. Nat. Med. *15*, 750–756.

Förch, P., Puig, O., Kedersha, N., Martínez, C., Granneman, S., Séraphin, B., Anderson, P., and Valcárcel, J. (2000). The apoptosis-promoting factor TIA-1 is a regulator of alternative pre-mRNA splicing. Mol. Cell *6*, 1089–1098.

Förch, P., Puig, O., Martínez, C., Séraphin, B., and Valcárcel, J. (2002). The splicing regulator TIA-1 interacts with U1-C to promote U1 snRNP recruitment to 5′ splice sites. EMBO J. *21*, 6882–6892.

Gelfman, S., Burstein, D., Penn, O., Savchenko, A., Amit, M., Schwartz, S., Pupko, T., and Ast, G. (2012). Changes in exon-intron structure during vertebrate evolution affect the splicing pattern of exons. Genome Res. *22*, 35–50.

Hoell, J.I., Larsson, E., Runge, S., Nusbaum, J.D., Duggimpudi, S., Farazi, T.A., Hafner, M., Borkhardt, A., Sander, C., and Tuschl, T. (2011). RNA targets of wild-type and mutant FET family proteins. Nat. Struct. Mol. Biol. *18*, 1428–1431.

Izquierdo, J.M., Majós, N., Bonnal, S., Martínez, C., Castelo, R., Guigó, R., Bilbao, D., and Valcárcel, J. (2005). Regulation of Fas alternative splicing by antagonistic effects of TIA-1 and PTB on exon definition. Mol. Cell *19*, 475–484.

Jamison, S.F., Pasman, Z., Wang, J., Will, C., Lührmann, R., Manley, J.L., and Garcia-Blanco, M.A. (1995). U1 snRNP-ASF/SF2 interaction and 5′ splice site recognition: characterization of required elements. Nucleic Acids Res. *23*, 3260–3267.

Knoop, L.L., and Baker, S.J. (2000). The splicing factor U1C represses EWS/FLI-mediated transactivation. J. Biol. Chem. *275*, 24865–24871.

Knoop, L.L., and Baker, S.J. (2001). EWS/FLI alters 5′-splice site selection. J. Biol. Chem. *276*, 22317–22322.

Kohtz, J.D., Jamison, S.F., Will, C.L., Zuo, P., Lührmann, R., Garcia-Blanco, M.A., and Manley, J.L. (1994). Protein-protein interactions and 5′-splice-site recognition in mammalian mRNA precursors. Nature *368*, 119–124.

Kornblihtt, A.R. (2007). Coupling transcription and alternative splicing. Adv. Exp. Med. Biol. *623*, 175–189.

Lerga, A., Hallier, M., Delva, L., Orvain, C., Gallais, I., Marie, J., and Moreau-Gachelin, F. (2001). Identification of an RNA binding specificity for the potential splicing factor TLS. J. Biol. Chem. *276*, 6807–6816.

Marco-Sola, S., Sammeth, M., Guigó, R., and Ribeca, P. (2012). The GEM mapper: fast, accurate and versatile alignment by filtration. Nat. Methods *9*, 1185–1188.

Mountz, J.D., Zhou, T., Wu, J., Wang, W., Su, X., and Cheng, J. (1995). Regulation of apoptosis in immune cells. J. Clin. Immunol. *15*, 1–16.

Ohno, T., Ouchida, M., Lee, L., Gatalica, Z., Rao, V.N., and Reddy, E.S. (1994). The EWS gene, involved in Ewing family of tumors, malignant melanoma of soft parts and desmoplastic small round cell tumors, codes for an RNA binding protein with novel regulatory domains. Oncogene *9*, 3087–3097.

Paronetto, M.P. (2013). Ewing Sarcoma Protein: A Key Player in Human Cancer. Int. J. Cell Biol. *2013*, 642853.

Paronetto, M.P., Miñana, B., and Valcárcel, J. (2011). The Ewing sarcoma protein regulates DNA damage-induced alternative splicing. Mol. Cell *43*, 353–368.

Ross, K.A., Smyth, N.A., Murawski, C.D., and Kennedy, J.G. (2013). The biology of ewing sarcoma. ISRN Oncol *2013*, 759725.

Sanchez, G., Bittencourt, D., Laud, K., Barbier, J., Delattre, O., Auboeuf, D., and Dutertre, M. (2008). Alteration of cyclin D1 transcript elongation by a

mutated transcription factor up-regulates the oncogenic D1b splice isoform in cancer. Proc. Natl. Acad. Sci. USA *105*, 6004–6009.

Takahama, K., Kino, K., Arai, S., Kurokawa, R., and Oyoshi, T. (2011). Identification of Ewing's sarcoma protein as a G-quadruplex DNA- and RNA-binding protein. FEBS J. *278*, 988–998.

Tan, A.Y., and Manley, J.L. (2009). The TET family of proteins: functions and roles in disease. J. Mol. Cell Biol. *1*, 82–92.

Wahl, M.C., Will, C.L., and Lührmann, R. (2009). The spliceosome: design principles of a dynamic RNP machine. Cell *136*, 701–718.

Wang, Z., Kayikci, M., Briese, M., Zarnack, K., Luscombe, N.M., Rot, G., Zupan, B., Curk, T., and Ule, J. (2010). iCLIP predicts the dual splicing effects of TIA-RNA interactions. PLoS Biol. *8*, e1000530.

Witten, J.T., and Ule, J. (2011). Understanding splicing regulation through RNA splicing maps. Trends Genet. *27*, 89–97.

Xiao, X., Wang, Z., Jang, M., Nutiu, R., Wang, E.T., and Burge, C.B. (2009). Splice site strength-dependent activity and genetic buffering by poly-G runs. Nat. Struct. Mol. Biol. *16*, 1094–1100.

Yeo, G., and Burge, C.B. (2004). Maximum entropy modeling of short sequence motifs with applications to RNA splicing signals. J. Comput. Biol. *11*, 377–394.

Zhang, D., Paley, A.J., and Childs, G. (1998). The transcriptional repressor ZFM1 interacts with and modulates the ability of EWS to activate transcription. J. Biol. Chem. *273*, 18086–18091.